2024 18th International Conference on
Control, Automation, Robotics and Vision (ICARCV)
December 12-15, 2024. Dubai

Motion Planning for Quadrupled Teams: An Experimental Evaluation Using a Dynamic Fluid Flow Model

Mohammad Ghufran, Sourish Tetakayala, and Hossein Rastgoftar

Abstract— **This paper applies the principles of fluid mechanics to develop a new method for motion planning in contented environments where multiple groups of agents want to reach their target while guaranteeing inter-agent collision avoidance. Assuming M groups of agents exist in the same motion space, we propose a time-varying ideal fluid flow model to safely plan the desired coordination of each group in the presence of other groups that are considered singularity points in the fluid flow field. To ensure that each group reaches its target destination, we propose to define the desired trajectory of each group along the streamlines of the fluid field but continuously direct the streamlines toward the target destination. The proposed solution, is experimentally evaluated by using quadruped robots in an indoor robotic facility.**

I. Introduction

Multi-robot systems, particularly those involving quadruped robots, have gained significant attention in recent years due to their potential applications in various domains, such as search and rescue, exploration, and transportation. One of the key challenges in deploying a team of quadruped robots is ensuring collision-free motion while navigating complex and dynamic environments. Traditional path planning and collision avoidance techniques often struggle to cope with multi-robot systems' high-dimensional and real-time constraints.

A. Related Work

The control and robotics communities have actively investigated multi-agent collision avoidance in the past few decades. Control Barrier Function (CBF) is an available method that has been widely accepted to ensure safety and collision avoidance [1], [2]. CBF has been mainly applied to control affine systems to describe the admissible Lipschitz continuous controls that guarantee forward invariance over a given safety zone. CBF designs the agent's control inputs such that the robot's state always stays inside the acceptable zone, which is defined by system dynamics in the CBF workspace. In [1], CBF is experimentally evaluated by using quadrotors and compared with artificial potential field [3], [4] as another method for ensuring inter-agent collision avoidance. In [5], CBF is applied to ensure safe and autonomous coordination in an unknown environment.

LaValle's seminal work on planning algorithms provides a in depth survey of various path planning techniques; this study was the early stages which now serves as foundational techniques for multi-robot navigation [6]. The sampling-based algorithms developed by Karaman and Frazzoli have demonstrated the capability of the robots in complex environments, highlighting the robustness of these methods in handling high-dimensional spaces. [7]. The implementation of motion planning with dynamic obstacles in real time navigation [8] by reif and Wang provides insights of its challenges. Schwager proposed a framework which is close to dynamic fluid flow-based navigation [9].

Recent studies have further developed the capabilities of multi-robot control strategies. Kantaros and Zavlanos have worked with reinforcement learning for multi-robotic systems; this approach enhances the adaptability of heterogeneous robots in dynamic environments [10]. Cheng has presented his work with deep learning of decentralised multi-robot navigation in complex environments which had efficient path planning [11]. The capacity of the multi-robots to traverse safely in densely crowded regions was demonstrated by Everett et al.'s work on collision avoidance utilizing deep reinforcement learning [12]. Specially for the quadruped robots, A broad research have been conducted to improve the mobility and control through different environments . Hutter introduced ANYmal, designed a quadruped robot which has high mobility in rough environments , displaying the improvements in the field [13]. The dynamic fluid-flow approach for robotic swarms proposed by Dia Paola, The theoretical approach that inspires the navigation model in this paper [14]. A recent study by Yang focused on a model predictive control for quadruped robots by improving stability and agility [15].

B. Contributions

In this paper, we present a collision-free quadruped team motion approach based on a dynamic fluid flow navigation model. Inspired by analytical solution for ideal fluid flow over multiple cylinders [16]–[19], we propose to consider robots as particles in fluid flow with streamlines that safely wrap obstacles. Particularly, we apply a dynamic ideal fluid flow model where the potential and stream fields of the fluid flow can be dynamically shaped to ensure that agents reach their targets in a contested and obstacle-laden environments, while gents are restricted to sliding along the streamlines at any time.

Compared to the CBF approach [20]–[23], we propose a novel model-free collision avoidance method that treats each obstacle as a "rigid body" whose boundary is determined by a streamline enclosing it. Therefore, boundaries enclosing obstacles are not trespassed when desired trajectories are

Authors are with the Aerospace and Mechanical Engineering Department, University of Arizona, Tucson, Arizona, USA, {ghufran1942, sourish, hrastgoftar}@arizona.edu

defined along the streamlines generated by solving a Laplace partial differential equation (PDE) over an obstacle-laden motion space.

To validate the effectiveness of the proposed approach, real-world experiments are conducted using quadruped robots in the Scalable Move and Resilient Traversability (SMART) lab. The Vicon motion capture providing real-time position data plays a major role in keeping track of the robots position and reducing the error between its current position and desired position. These experiments analyze the systems performance in maintaining collision-free navigation following intended trajectories, despite the presence of obstacles and dynamic interactions between the robots. Compared to the existing literature and the authors' previous work, this paper offers the following novel contributions:

1) Development of a dynamic fluid flow navigation model for multi-robot systems.
2) Implementing real-time control, under the fluid flow guidance model, with Robot Operation System 2 (ROS2) for communication and coordination.
3) Validation of the model with real-world experiments with multiple quadruped robots.
4) Demonstration of the systems effectiveness in maintaining collision-free navigation by following the intended trajectory.

C. Outline

The remainder of this paper is organized as follows: Section II presents the proposed dynamic fluid flow navigation model and its mathematical formulation. Section III describes an overview of the system control. Section IV describes the simulation setup and experimental methodology. Section V presents and discusses the results obtained from simulations and real-world experiments. Finally, Section VI concludes the paper and outlines future research directions.

II. Methodology

We consider m groups of agents identified by $\mathcal{V}_1$ through $\mathcal{V}_m$ moving in the same motion space. We use set $\mathcal{M} = \{1, \cdots, m\}$ to define the agent identification numbers. To abstractly specify our motion planning model, we use $\mathcal{V}_l$ to identify the quadrupeds that belong to $l \in \mathcal{M}$ and $\bar{\mathcal{V}}_l$ to define any other (stationary or dynamic) agent in the motion space.

We apply the ideal fluid flow model to safely plan motion of $\mathcal{V}_l$'s agents in the presence of $\bar{\mathcal{V}}_l$'s agents, for every $l \in \mathcal{M}$. We note that $\bar{\mathcal{V}}_l$ define both stationary and dynamic agents where stationary agents can represent obstacles. More specifically, we consider $\mathcal{V}_l$'s agents as particles of a dynamics ideal fluid flow field that always slide along the streamlines, where every other agent belonging to $\bar{\mathcal{V}}_l$ is considered a singularity point and safely excluded by an streamline for the fluid flow field.

To apply the fluid flow model, we define ϕ_l and ψ_l over the $x-y$ plane as the potential and stream functions used for modeling the motion of group $l \in \mathcal{M}$ where both field

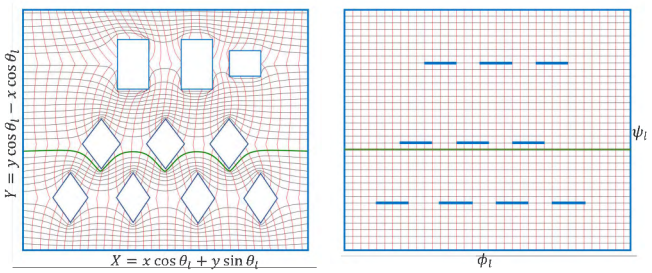

Fig. 1: *Left:* Motion space with streamlines shown by black and potential lines shown by red. *Right:* $\phi_l - \psi_l$ plane.

functions satisfy the Laplace partial differential equation:

$$\frac{\partial^2 \phi_l}{\partial x^2} + \frac{\partial^2 \phi_l}{\partial y^2} = 0, \qquad l \in \mathcal{M}, \tag{1a}$$

$$\frac{\partial^2 \psi_l}{\partial x^2} + \frac{\partial^2 \psi_l}{\partial y^2} = 0, \qquad l \in \mathcal{M}. \tag{1b}$$

By defining motion planning as an ideal fluid flow coordination, we indeed establish a mapping between the $x-y$ plane and $\phi_l - \psi_l$ plane where obstacles in the where obstacles in the motion space are mapped line segments that cannot be crossed (see Fig. 1). Level curves ϕ_l-constant and ψ_l-constant are orthogonal at every intersection point in the $x-y$ plane.

In this paper, complex variable $\mathbf{z} = x + \mathbf{j}y$ is used to denote position in the motion space because we consider coordination of quadruped robots over a 2-D plane. To be more precise, we use the complex variable $\mathbf{z}_i = x_i + \mathbf{j}y_i$ to denote the desired position of agent $i \in \mathcal{V}_l$ and $\mathbf{z}_h = x_h + \mathbf{j}y_h$ to denote the nominal position of agent $h \in \bar{\mathcal{V}}_l$, for $l \in \mathcal{M}$. To safely plan $\mathcal{V}_l$'s agent motion, in the presence of $\bar{\mathcal{V}}_l$'s agents, we consider the following requirements for specifying ϕ_l and ψ_l:

1) **Requirement 1:** Every agent $i \in \mathcal{V}_l$ must slide along stream function ψ_l.
2) **Requirement 2:** Every $\bar{\mathcal{V}}_l$ is considered as a singularity point of ideal fluid flow field specified for group $l \in \mathcal{M}$ and safely enclosed by a level curve ψ-constant.
3) **Requirement 3:** The potential and stream field ϕ_l and ψ_l are dynamically shaped so that $\mathcal{V}_l$'s agents ultimately reach their target positions.

To achieve Requirements 1, 2, and 3, we define ϕ_l and ψ_l as the real and imaginary part of analytic function

$$\begin{aligned}\mathbf{f}\left(\mathbf{z}_i e^{-\mathbf{j}\theta_l(t)}, t\right) &= \phi_l(x_i, y_i, \theta_l(t), t) + \mathbf{j}\psi_l(x_i, y_i, \theta_l(t), t) \\ &= (1-\beta_l)\,\mathbf{z}_i e^{-\mathbf{j}\theta_l} + \beta_l \sum_{h \in \bar{\mathcal{V}}_l} \left(\left(\mathbf{z}_i e^{-\mathbf{j}\theta_l} - \mathbf{z}_h(t)\right) + \frac{\Delta_h^2}{\mathbf{z}_i e^{-\mathbf{j}\theta_l} - \mathbf{z}_h(t)} \right),\end{aligned} \tag{2}$$

where $\beta_l \in \{0, 1\}$ takes 0 if motion $\bar{\mathcal{V}}_l$'s agents do not influence the motion of $\mathcal{V}_l$'s agents, and 1 otherwise. Also, parameter Δ_h is used to adjust the size of the domain enclosing agent $h \in \mathcal{V}_l$, for $l \in \mathcal{M}$. In addition, $\theta_l(t)$ establishes the nominal motion direction of $\mathcal{V}_l$'s agents and updates the stream lines to form the group $l \in \mathcal{M}$'s motion direction in

the direction of their intended destination at any given time t. Note that θ_l can be either constant or time-varying. Constant θ_l is computed based on initial and target destinations of $\mathcal{V}_l$'s agents. More specifically, we use $\mathbf{Z}_{0,l} = X_{0,l} + \mathbf{j}Y_{0,l}$ and $\mathbf{Z}_{f,l} = X_{f,l} + \mathbf{j}Y_{f,l}$ to denote the given initial and final positions of every group $l \in \mathcal{M}$ and obtain constant θ_l by

$$\theta_l = \tan^{-1}\left(\frac{Y_{f,l} - Y_{0,l}}{X_{f,l} - X_{0,l}}\right), \qquad l \in \mathcal{M}, \tag{3}$$

Time-varying θ_l is obtained based on the current and final nominal positions of the $\mathcal{V}_l$'s agents by

$$\theta_l(t) = \tan^{-1}\left(\frac{Y_{f,l} - \bar{y}_l(t)}{X_{f,l} - \bar{x}_l(t)}\right), \qquad l \in \mathcal{M}, \tag{4}$$

where

$$\bar{x}_l(t) = \frac{1}{|\mathcal{V}_l|}\sum_{i\in\mathcal{V}_l} x_i(t), \qquad l \in \mathcal{M}, \tag{5a}$$

$$\bar{y}_l(t) = \frac{1}{|\mathcal{V}_l|}\sum_{i\in\mathcal{V}_l} y_i(t), \qquad l \in \mathcal{M}. \tag{5b}$$

We desire that $\mathcal{V}_l$'s agents slide along a streamline where $\bar{\mathcal{V}}_l$'s agents are the singularity points of the fluid flow field and safely wrapped. Consequently, desired position of agent $i \in \mathcal{V}_l$ is obtained by

$$x_i = g_1(\phi_{il}, \psi_{il}, \theta_l, t), \qquad \forall i \in \mathcal{V}_l,\ l \in \mathcal{M}, \tag{6a}$$

$$y_i = g_2(\phi_{il}, \psi_{il}, \theta_l, t), \qquad \forall i \in \mathcal{V}_l,\ l \in \mathcal{M}, \tag{6b}$$

where $\phi_{il} = \phi_l(x_i, y_i, \theta_l(t), t)$ and $\psi_{il} = \psi_l(x_i, y_i, \theta_l(t), t)$ denote the potential and stream coordinates of agent $i \in \mathcal{V}_l$, g_1 and g_2 are non-singular and map $\phi_l - \psi_l$ to $x - y$ plane given θ_l and positions of $\bar{\mathcal{V}}_l$'s agents. Also,

$$\hat{\mathbf{T}}_i = \begin{bmatrix} \dfrac{\partial \psi_l(x_i, y_i, \theta_l, t)}{\partial y} & -\dfrac{\partial \psi_l(x_i, y_i, \theta_l, t)}{\partial x} \end{bmatrix}^T, \tag{7}$$

is the vector tangent specifying the motion direction of every agent $i \in \mathcal{V}_l$. To obtain the desired trajectory of every agent $i \in \mathcal{V}_l$ the sliding speed along streamline $\psi_{il} =$ constant is the same for every agent $i \in \mathcal{V}_l$ ($l \in \mathcal{M}$). Therefore, potential coordinate ϕ_{il} is updated by

$$\phi_{il}(t_{k+1}) = \phi_{il}(t_k) + d\phi_l, \qquad \forall i \in \mathcal{V}_l,\ l \in \mathcal{M},\ k = 1, 2, \cdots, \tag{8}$$

where t_k is discrte, time $t_{k+1} = t_k + \Delta t$, and Δt is a constant time increment.

Remark 1. Both time-varying potential and stream fields obtained by (2) satisfy the Laplace PDE that implies that

$$\frac{\partial^2 \phi_l(x_i, y_i, \theta_l(t), t)}{\partial x_i^2} + \frac{\partial^2 \phi_l(x_i, y_i, \theta_l(t), t)}{\partial y_i^2} = 0, \qquad l \in \mathcal{M}, \tag{9a}$$

$$\frac{\partial^2 \psi_l(x_i, y_i, \theta_l(t), t)}{\partial x_i^2} + \frac{\partial^2 \psi_l(x_i, y_i, \theta_l(t), t)}{\partial y_i^2} = 0, \qquad l \in \mathcal{M}, \tag{9b}$$

for every $i \in \mathcal{V}_l$ at any time t given any value of $\theta_l \in [0, 2\pi)$.

In this paper, we experimentally evaluate the proposed fluid flow coordination model by using quadruped agents under three scenarios that include Single Group Free Environment (SGFE), Single Group Obstacle-Laden Environment (SGOLE), and Cooperative Time-Varying Environment (CTVE). The properties of these experiments are listed in I.

TABLE I: Design parameters for every agent group $l \in \mathcal{M}$ under different experiments

Experiment	θ_l	β_l	$\lvert\mathcal{M}\rvert$
SGFE	constant	0	1
SGOLE	constant	1	1
CTVE	time-varying	1	≥ 1

Algorithm 1 Algorithm for dynamic fluid-flow coordination of $\mathcal{V}_l$'s agents when $\bar{\mathcal{V}}_l$'s are stationary, for $l \in \mathcal{M}$.

Get: Initial and finial positions of every $i \in \mathcal{V}_l$ and nominal position of every agent $h \in \bar{\mathcal{V}}_l$; $d\phi_l$; Δ_h for every $h \in \bar{\mathcal{V}}_l$; small $\epsilon > 0$; time increment Δt.
Obtain θ_l by Eq. (3).
Obtain $\phi_{i,l}$ and ψ_{il} by Eq. (2) for every $i \in \mathcal{V}_l$
Set $check = 0$ and $k = 0$.
Define time $t_k = 0$.
while $check = 0$ **do**
  for $i \in \mathcal{V}_l$ **do**
    Obtain $\phi_{i,l}$ and ψ_{il} by Eq. (2).
    $\phi_{i,l} \leftarrow \phi_{i,l} + d\phi_l$.
    Obtain $x_i(t_k)$ and $y_i(t_k)$ by (6a) and (6b).
  end for
  $k \leftarrow k + 1$.
  $t_k \leftarrow t_{k-1} + \Delta t$.
  Obtain $x_i(t_k)$ and $y_i(t_k)$ by (6a) and (6b).
  Update $\bar{x}_l(t_k)$ and $\bar{y}_l(t_k)$ using Eq. (5).
  if $|(\bar{x}_l(t_k) - X_l) + \mathbf{j}(\bar{y}_l(t_k) - Y_l)| \leq \epsilon$ **then**
    $check \leftarrow check + 1$.
  end if
end while

For the SGFE experiment, no obstacle exists in the motion space, therefore, $\beta_l = 0$ and $|\mathcal{M}| = 1$. We use $\theta_1 = \theta$, $\phi_1 = \phi$, $\psi_1 = \psi$, $\mathcal{V}_1 = \mathcal{V}$ to specify motion planning properties, where the potential and streamlines, applied to plan motion of the $\mathcal{V}$'s agents, simplify to

$$\phi(x_i, y_i, \theta) = x_i \cos\theta + y_i \sin\theta, \qquad i \in \mathcal{V}, \tag{10a}$$

$$\psi(x_i, y_i, \theta) = -x_i \sin\theta + y_i \cos\theta, \qquad i \in \mathcal{V}, \tag{10b}$$

Note that θ is constant and obtained by Eq. (3) for the SGFE experiment.

In the SGOLE experiment, $\bar{\mathcal{V}}_l$'s agents are stationary; therefore, $\mathbf{z}_h$ is constant for every $h \in \bar{\mathcal{V}}_l$ and $l \in \mathcal{M}$, and constant θ_l given by Eq. (3) is used at any time t. Additionally, the fluid flow coordination's potential and stream functions, as determined by Eq. (2), are solely spatially-varying. For SGOLE, we use Algorithm 1 to safely plan agents' desired trajectories.

In the CTVE experiment, we consider multiple groups of agents that cooperatively plan their desired trajectories by

shaping the stream lines allocated to every agent $i \in \mathcal{V}_l$ so that each group reaches the desired nominal final location, where $\theta_l(t)$ is updated by Eq. (4) at any time t, for every $l \in \mathcal{M}$. For CTVE, we apply Algorithm 2 to plan the desired trajectories of all agents.

Algorithm 2 Algorithm for dynamic fluid-flow coordination of $\mathcal{V}_l$'s agents when $\bar{\mathcal{V}}_l$'s are stationary, for $l \in \mathcal{M}$.

Get: Initial and finial positions of every $i \in \mathcal{V}_l$ and nominal position of every agent $h \in \bar{\mathcal{V}}_l$; $d\phi_l$; Δ_h for every $h \in \bar{\mathcal{V}}_l$; small $\epsilon > 0$; time increment Δt.
Set $check_l = 0$, for every $l \in \mathcal{M}$, and $k = 0$.
Define time $t_k = 0$.
for $l \in \mathcal{M}$ **do**
  while $check_l = 0$ **do**
    for $i \in \mathcal{V}_l$ **do**
      Obtain θ_l by Eq. (4).
      Obtain $\phi_{i,l}$ and ψ_{il} by Eq. (2).
      Updade $\phi_{i,l} \leftarrow \phi_{i,l} + d\phi_l$.
      Obtain $x_i(t_k)$ and $y_i(t_k)$ by (6a) and (6b).
    end for
    $k \leftarrow k+1$.
    $t_k \leftarrow t_{k-1} + \Delta t$.
    Update $\bar{x}_l$ and $\bar{y}_l$ using Eq. (5).
    if $|(\bar{x}_l - X_l) + \mathbf{j}(\bar{y}_l - Y_l)| \leq \epsilon$ **then**
      $check_l \leftarrow check_l + 1$.
    end if
  end while
end for

III. System Control

The Unitree Go1 is controlled using high level control provided by Unitree SDK with ROS2 as the communication protocol. The high level control involves executing a selected movement method from a predefined array of movements methods such as idle, stand up, walking, and recovery etc. The use of ROS2 allows seamless communication between the Go1 and other devices like Vicon for positioning that we are using with the II, ensuring precise control and adjustment of movements in real-time. The use of Vicon helps in serving the quadrupeds with precise position and orientation.

We utilized a ROS2 node that manages the agent's direction, speed, and movement method based on the way-points generated by algorithm 1 and 2. By analyzing the current position and the next way-points, it dynamically adjust the robot's high level parameters to ensure smooth and efficient navigation.

IV. Experimental Setup

The experiments were performed indoor experimental space available at the SMART lab to conduct our experiment. The overview of the experiment is illustrated in Fig. 2. The experimental setup includes (i) two quadrupeds (ii) a motion capture system (Vicon), and (iii) a ground control center are described below.

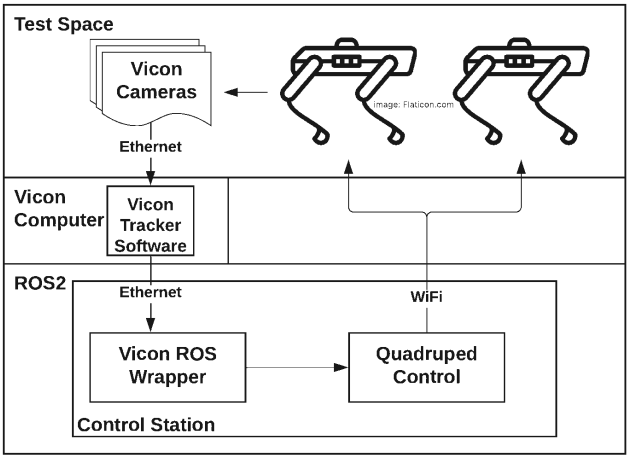

Fig. 2: System overview

A. Unitree Go1 Robots

For the experiments, we utilized two Unitree Go1 robots as they are robust and agile. Both the robots are equipped with standard sensors and reflective markers to ensure precise tracking by Vicon motion capture system. The integration of ROS2 makes the communication and data handling seamless, using ROS2's Publishers and subscribers to manage high-level commands (`/HighCmd`) and subscribe to positional data from the Vicon system.

B. Vicon Motion Capture System

The Lab is equipped with an eight camera's network to maximise the tracking area and eliminate blind spots. Each Unitree Go 1 is fitted with 4-6 markers, enabling accurate observation of the position and orientation of the object. The Vicon system data is transmitted to a ground system computer(GCS). The gathered data is transferred to a Vicon receiver through Ethernet for utilization.

C. Ground Control Station (GCS)

The ground control station utilizes the incoming vicon data from the vicon computer and implements the methodology (Section II) using algorithm 1 and 2. The GCS ensures real-time control through active agent callback, updating the agent positions and orientations, and adjusting their movement to maintain the intended trajectory.

V. Experimental Results

We experimentally validated our results by utilizing two quadrupeds.The experiments were performed in the Scalable Move and Resilient Transversality (SMART) Lab at the University of Arizona. The facility has an indoor operational area measuring 5m × 5m × 2m equipped with 8 VICON motion capture cameras. To ensure controlled testing conditions, we confined the quadruped within this space.

A. SGFE Experiment

For the SGFE experiment, as single group of quadruped robots, defined by $\mathcal{V} = \{1,2\}$ moves in an obstacle-free motion space when $\bar{\mathcal{V}} = \emptyset$. Given initial and target location of the quadruped robot team, shown in Fig. 4 the desired paths of the two quadruped robots based on the potential and stream fields obtained by Eq. 4. The actual and desired paths of the quadruped robots are shown by dashed and continuous plots in Fig. 4.

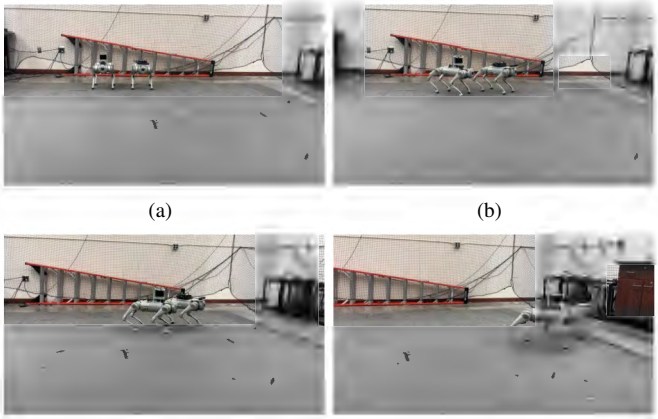

(a) (b) (c) (d)

Fig. 3: Experiment 1 (SGFE): Configurations of the Quadruped robots at different times.

B. SGOLE Experiment

For the SGOLE experiment, we defined a static obstacle at $(x, y) = (0,0)$. The goal of the experiment is to validate the methodology outlined in Section II for static object. The position and orientation of the groups and the object are integrated into the algorithm with the help of the Vicon ROS2 wrapper and the Vicon software.

As shown in the Fig. 6, the implementation of the proposed methodology(II) using algorithm 1, demonstrates that the quadrupeds effectively avoid the object present in the motion space. Fig. 5 illustrates the various configurations that the agents go through to achieve the desired result.

C. CTVE Experiment

In the second experiment, group 1 treats group 2 as an anomaly, and vice versa. The aim of this experiment is to validate the methodology described in Section II for dynamic objects. More specifically, we use $\mathcal{V}_1 = \{1\}$ and $\mathcal{V}_2 = \{2\}$ to define the quadruped robots where $\bar{\mathcal{V}}_1 = \mathcal{V}_2$ and $\bar{\mathcal{V}}_2 = \mathcal{V}_1$. For safe motion planning of the quadruped we use Algorithm 2 to receive the current position of both the groups in real time using ROS2. In Fig. 8, we can see that the agents avoid each other in the motion space without colliding. This demonstrates that the methodology is effective for both dynamic and static objects. Fig. 7 shows the different configuration of the agents at various time interval.

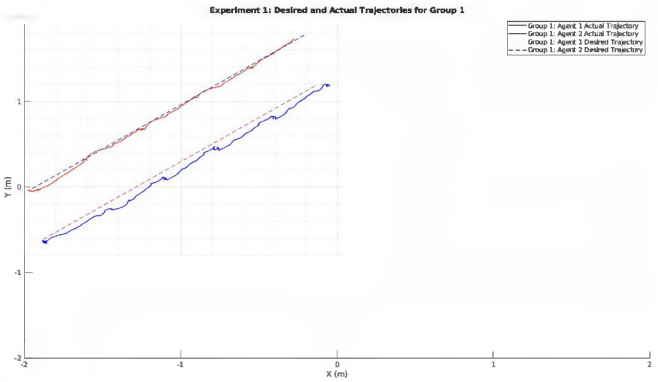

Fig. 4: Desired and actual paths of the quadruped robots in the SGFE experiment shown by dashed and continuous curves.

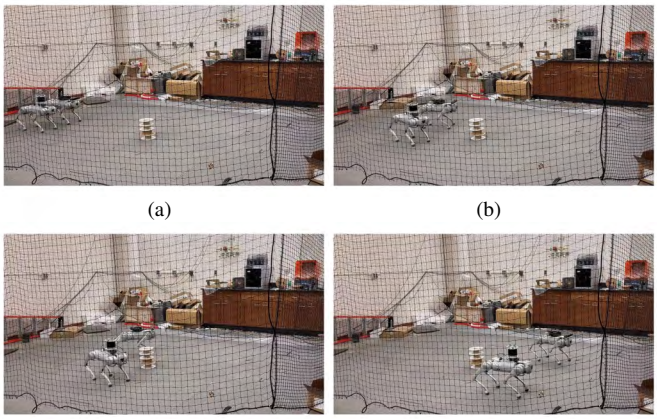

(a) (b) (c) (d)

Fig. 5: Experiment 2 (SGOLE): Configurations of the Quadruped robots at different time

VI. Conclusion

In this work, we applied the principles of fluid flow to develop a method for motion planning of multiple groups in an obstacle-laden environment while avoiding each other. The methodology presented in Section II was experimentally validated at the SMART Lab of the University of Arizona using quadrupeds for both stationary and dynamic objects. For future work, we plan to incorporate object detection algorithms for identifying objects and use the Global Positioning System (GPS) for positioning instead of Vicon, as used in this work. Specifically, we aim to use the Yolo Algorithm for object identification and methods to identify other groups in the motion space, while leveraging GPS for accurate outdoor positioning.

References

[1] A. Singletary, K. Klingebiel, J. Bourne, A. Browning, P. Tokumaru, and A. Ames, "Comparative analysis of control barrier functions and artificial potential fields for obstacle avoidance," in *2021 IEEE/RSJ International Conference on Intelligent Robots and Systems (IROS)*. IEEE, 2021, pp. 8129–8136.

[2] Y. Chen, H. Peng, and J. Grizzle, "Obstacle avoidance for low-speed autonomous vehicles with barrier function," *IEEE Transactions on Control Systems Technology*, vol. 26, no. 1, pp. 194–206, 2017.

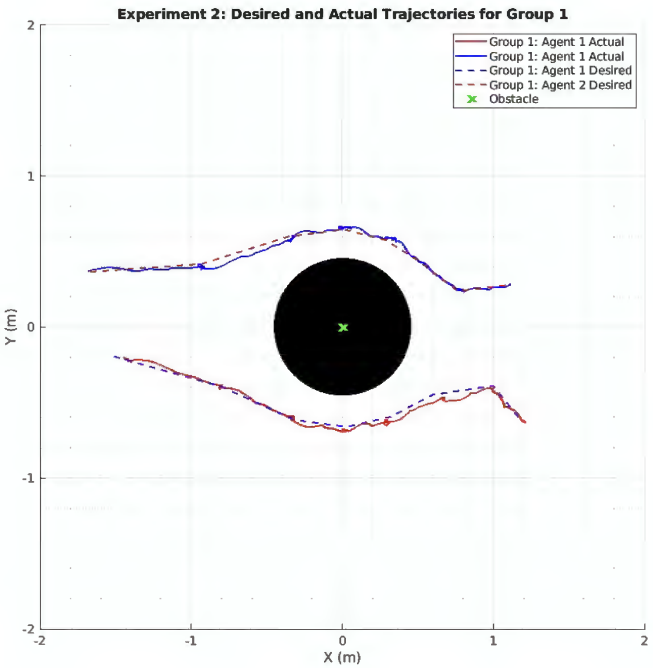

Fig. 6: Desired and actual paths of the quadruped robots in the SGOLE experiment shown by dashed and continuous curves.

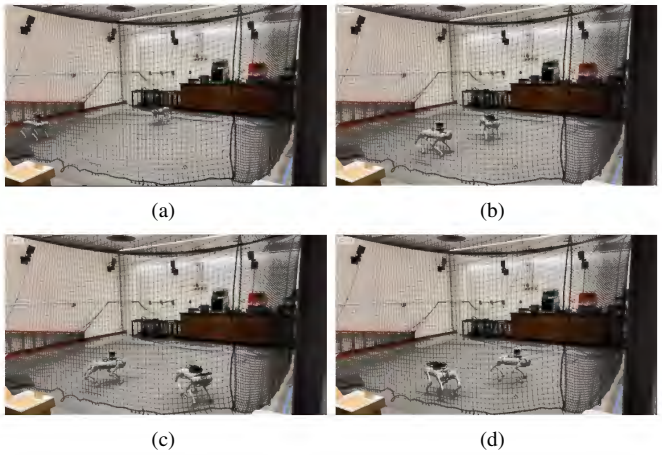

(a) (b)

(c) (d)

Fig. 7: Experiment 3 (CTVE): Configurations of the Quadruped robots at different time

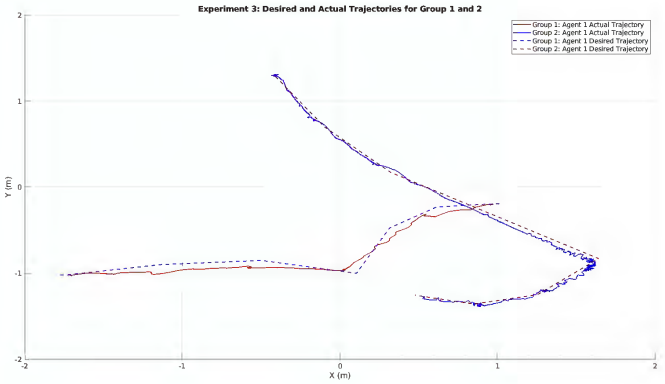

Fig. 8: Desired and actual paths of the quadruped robots in the CTVE experiment shown by dashed and continuous curves.

[3] M. T. Wolf and J. W. Burdick, "Artificial potential functions for highway driving with collision avoidance," in *2008 IEEE International Conference on Robotics and Automation*. IEEE, 2008, pp. 3731–3736.

[4] E. G. Hernández-Martínez, E. Aranda-Bricaire, F. Alkhateeb, E. Maghayreh, and I. Doush, "Convergence and collision avoidance in formation control: A survey of the artificial potential functions approach," *Multi-agent systems—modeling, control, programming, simulations and applications*, pp. 103–126, 2011.

[5] C. Li, Z. Zhang, A. Nesrin, Q. Liu, F. Liu, and M. Buss, "Instantaneous local control barrier function: An online learning approach for collision avoidance," *arXiv preprint arXiv:2106.05341*, 2021.

[6] S. M. LaValle, *Planning algorithms*. Cambridge university press, 2006.

[7] S. Karaman and E. Frazzoli, "Sampling-based algorithms for optimal motion planning," *The international journal of robotics research*, vol. 30, no. 7, pp. 846–894, 2011.

[8] J. H. Reif and H. Wang, "Motion planning in the presence of moving obstacles," *Algorithmica*, vol. 10, no. 1, pp. 514–547, 1999.

[9] M. Schwager, D. Rus, and J.-J. E. Slotine, "A unifying framework for modeling and controlling cooperative multi-robot systems," *Proceedings of the IEEE*, vol. 100, no. 13, pp. 345–364, 2011.

[10] Y. Kantaros and M. M. Zavlanos, "Distributed reinforcement learning for multi-robot systems," *IEEE Transactions on Robotics*, vol. 35, no. 4, pp. 971–988, 2019.

[11] Y. F. Chen, M. Liu, and M. Tomizuka, "Decentralized multi-robot navigation in complex environments using deep learning," *IEEE Robotics and Automation Letters*, vol. 5, no. 2, pp. 2551–2558, 2020.

[12] M. Everett, Y. F. Chen, and J. P. How, "Collision avoidance in pedestrian-rich environments with deep reinforcement learning," *IEEE Transactions on Robotics*, vol. 34, no. 4, pp. 992–1003, 2018.

[13] M. Hutter, C. Gehring, D. Jud, A. Lauber, D. Bellicoso, V. Tsounis, J. Hwangbo, K. Bodie, P. Fankhauser, M. Bloesch *et al.*, "Anymal: A highly mobile and dynamic quadrupedal robot," *IEEE Robotics and Automation Letters*, vol. 3, no. 3, pp. 1800–1807, 2017.

[14] D. Di Paola, A. Tierno, and A. Martinoli, "Dynamic fluid-flow approach for robotic swarms," *Robotics and Autonomous Systems*, vol. 103, pp. 87–97, 2018.

[15] W. Yang, H. Ma, and V. Kumar, "Model predictive control for robust operation of quadrupedal robots," *The International Journal of Robotics Research*, vol. 39, no. 9, pp. 1118–1135, 2020.

[16] D. G. Crowdy, "Analytical solutions for uniform potential flow past multiple cylinders," *European Journal of Mechanics-B/Fluids*, vol. 25, no. 4, pp. 459–470, 2006.

[17] ——, "Uniform flow past a periodic array of cylinders," *European Journal of Mechanics-B/Fluids*, vol. 56, pp. 120–129, 2016.

[18] H. Rastgoftar and E. Atkins, "Physics-based freely scalable continuum deformation for uas traffic coordination," *IEEE Transactions on Control of Network Systems*, vol. 7, no. 2, pp. 532–544, 2019.

[19] H. Emadi, H. Uppaluru, H. Ashrafiuon, and H. Rastgoftar, "Collision-free continuum deformation coordination of a multi-quadcopter system using cooperative localization," in *2022 European Control Conference (ECC)*. IEEE, 2022, pp. 1349–1354.

[20] A. D. Ames, S. Coogan, M. Egerstedt, G. Notomista, K. Sreenath, and P. Tabuada, "Control barrier functions: Theory and applications," in *2019 18th European control conference (ECC)*. IEEE, 2019, pp. 3420–3431.

[21] A. D. Ames, J. W. Grizzle, and P. Tabuada, "Control barrier function based quadratic programs with application to adaptive cruise control," in *53rd IEEE Conference on Decision and Control*. IEEE, 2014, pp. 6271–6278.

[22] M. Jankovic, "Robust control barrier functions for constrained stabilization of nonlinear systems," *Automatica*, vol. 96, pp. 359–367, 2018.

[23] Y. Chen, A. Singletary, and A. D. Ames, "Guaranteed obstacle avoidance for multi-robot operations with limited actuation: A control barrier function approach," *IEEE Control Systems Letters*, vol. 5, no. 1, pp. 127–132, 2020.